Biophysical Chemistry 192 (2014) 27–32

Contents lists available at ScienceDirect

Biophysical Chemistry

journal homepage: http://www.elsevier.com/locate/biophyschem

Not all carboxylates are created equal: Differences in interaction of carboxylated peptides with a $CaCO_3$ dimer

Víctor M. Rosas-García *, Isidro de León-Abarte, Germán Vidal-López [1], Arturo Palacios-Pargas, Xóchitl Jáuregui-Prado

Facultad de Ciencias Químicas, Universidad Autónoma de Nuevo León, Ave. Manuel Barragán S/N, San Nicolás de los Garza, Nuevo León 66451, México

HIGHLIGHTS

- Carboxylated amino acids may show different affinities towards $CaCO_3$.
- $CaCO_3$ clusters reorganize upon binding to carboxylated side-chains.
- "Organic marshaling" is suggested as a concept for biomineralization control.
- Organic marshaling seems to withstand water solvation.

GRAPHICAL ABSTRACT

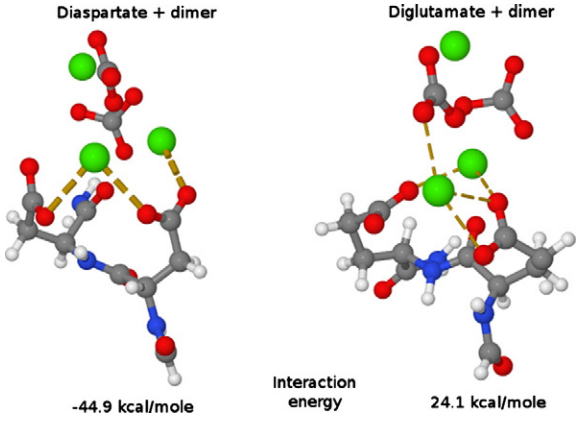

ARTICLE INFO

Article history:
Received 6 May 2014
Received in revised form 11 June 2014
Accepted 11 June 2014
Available online 21 June 2014

Keywords:
Asprich protein
Aggregation
Blind docking
Crystallization
Organic–inorganic interface

ABSTRACT

The carboxylate group has been considered the "glue" for mineralizing proteins because of its ability to bind Ca(II). We propose the calcium salts of dicarboxylated dipeptides (Asp-Asp and Glu-Glu) as the smallest models of a mineralizing protein active site. Molecular dynamics/simulated annealing was used for conformational search of the dipeptide global minimum. Semiempirical blind docking was used for configurational search of all cluster-peptide complexes and structures were then optimized in the gas phase at the RI-MP2/SVP level of theory. Solvent effects were also taken into account. We found that the energy of interaction of the calcium carboxylates with a calcium carbonate dimer can be either favorable or unfavorable depending on side-chain length, so side-chain carboxylic groups belonging to different amino acids may show different affinities towards calcium carbonate.

1. Introduction

One of the basic tenets of biomineralization is that organic molecules control nucleation and growth of bio-generated inorganic minerals [1]. Weiner was the first to propose the motif Asp-Y [2] as an essential building block for mineralizing proteins, due to the ability of the carboxylated side chain to bind calcium. Both aspartate and glutamate

* Corresponding author at: Universidad Autónoma de Nuevo León, Facultad de Ciencias Químicas, Ave. Manuel Barragán S/N, San Nicolás de los Garza, Nuevo León 66451, México. Tel.: +52 81 8329 4000x6253; fax: +52 81 8376 2929.
E-mail address: rosas.victor@gmail.com (V.M. Rosas-García).
[1] Present address: PIASA (Proveedores De Ingenieria Alimentaria S.A. de C.V.), Ave. Industrias #140, Esq. Privada Las Mitras, Fracc. PIMSA OTE, Parque Industrial Kronos, Apodaca, Nuevo León C.P. 66600, México.

http://dx.doi.org/10.1016/j.bpc.2014.06.003
0301-4622/

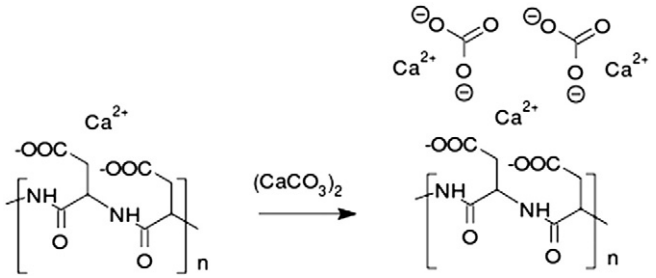

Fig. 1. Example of a proposed model of a biomineralizing site, using aspartate. The calcium dicarboxylate site functions as a scaffold for mineralization by binding calcium carbonate aggregates.

possess carboxylated side chains, and indeed, the participation of aspartate and glutamate in biomineralizing proteins is documented [3,4]. The carboxylate group has been considered the "glue of choice" for mineralizing proteins [5]. Despite this interest, up to this day, atomistic details of the biomineralization process are lacking. Even though both aspartate and glutamate have been found in mineralizing proteins, we lack information on the kind and strength of their interactions relevant to biomineralization. Polyacidic motifs have been found in mineralizing proteins such as human osteopontin [6] (with a motif comprising several diaspartate units: Asp-Asp-Met-Asp-Asp-Glu-Asp-Asp-Asp-Glu) and human bone sialoprotein [7] (with a motif composed of eight consecutive glutamates). For a review listing other examples of mineralizing proteins containing polyacidic motifs, see Gorski [8].

Among the studies of peptide interaction with $CaCO_3$, Gower and Odom [9] experimentally found that polyaspartate induces aggregation of calcium carbonate. Metzler et al. [4] have shown that carboxylate groups from aspartate and glutamate bind to growing $CaCO_3$ crystals. Chrissantopoulos computationally studied the interaction of calcium carbonate and polyglycine peptides [10] and found that the interaction was mostly with the ionized carboxylate group on the peptide C-terminus.

We do not need to restrict ourselves to crystal growth by single-ion aggregation. Navrotsky [11] suggested that a landscape of nanoparticle precursors offers a source of material for biomineralization. The structures of some of these $CaCO_3$ clusters were previously reported by us [12]. These nanoparticles and their precursors could be recognized by the mineralizing proteins and used for building biominerals.

We propose a "biomineralizing active site" consisting of two carboxylate groups binding a single calcium ion—in the manner proposed by Mann [13]—so the resulting active site is neutral and examine the energetics of the "smallest biomineralization event", that of a $CaCO_3$ dimer binding to this active site (see Fig. 1). We determine the active site of the dipeptide by looking for a region of the dipeptide that shows the most negative energy of binding to a calcium carbonate dimer. We then examine the variation in the strength of binding for calcium diaspartate and calcium diglutamate.

Table 1
Conformational minima for calcium diaspartate in the gas phase at the RI-MP2/SVP level of theory. The total electronic energy includes thermal corrections and zero point energy from vibrational analysis.

Conformer	Total electronic energy (Eh)	Relative energy (kcal/mol)
1	−1713.40447	0.00
2	−1713.39525	5.78
3	−1713.39478	6.08
4	−1713.39459	6.20
5	−1713.38909	9.65

2. Computational methods

To determine the relative orientation between a cluster and a peptide that yields the strongest interaction between the two, we have used a variation of blind docking [14]. In traditional blind-docking, a molecular mechanics force-field is used to evaluate the energy of interaction between two rigid molecules as their relative positions change using software such as AutoDock [15]. The main differences of our method are that we employed a semiempirical Hamiltonian instead of a molecular mechanics force-field; and instead of rigid molecules we allowed for structural relaxation by means of energy optimization. The relative positions and orientations were determined by software developed in-house.

We deem the electrostatic interaction observed by Chrissantopoulos [10] due to the ionized C-terminus carboxylate as an interference so, to avoid this, we capped both the C-terminus and the N-terminus turning them into amides by amidation and acetylation, respectively. This way, the only ionized groups in both diaspartate and diglutamate are the carboxylate groups present in the side chains.

Building and pre-optimization of molecular structures were done with the Tripos 5.2 [16] molecular mechanics force field as implemented in Ghemical v.2.99 [17]. Conformational search was done by the molecular dynamics facility provided in Ghemical. All the semiempirical calculations employed the PM6 [18] Hamiltonian as implemented in MOPAC2012 [19]. Optimizations at the RI-MP2 [20]/SVP [21] level of theory employed ORCA v.2.9 [22]. Vibrational frequency analyses revealed no imaginary frequencies and reported frequencies are unscaled. Interaction energies include zero-point energy and BSSE corrections. Aqueous solvation effects were considered by using the COSMO [23] solvent model. The use of this solvent model for the calculation of solvation energies of highly ionic species has been reported by Aziz et al. [24] for salts of carboxy acids using MP2/aug-cc-pVTZ—justifying our choice of MP2—and by Krossing et al. [25] for ionic liquids using (RI)-BP86/SV(P). In both cases COSMO was shown to adequately reproduce the trends in experimental solvation energies. The size of our systems precluded the use of a large basis set such as aug-cc-pVTZ, so we resorted to SVP. We also chose the RI formulation of MP2, as the difference with respect to standard MP2 is negligible [26].

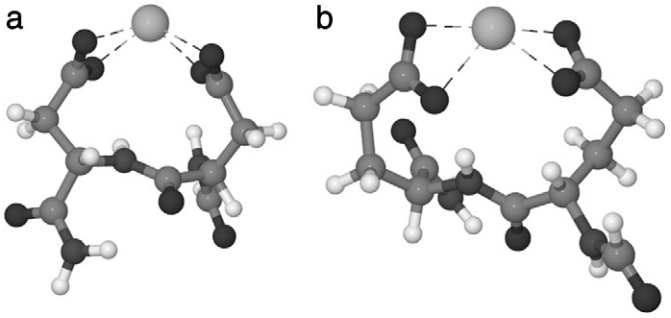

Fig. 2. Global minimum of calcium diaspartate (a) and calcium diglutamate (b) in the gas phase at the PM6 level of theory. The dotted lines indicate coordination between calcium and oxygen atoms. (Ca: light gray, O: black, N: dark gray, C: gray, H: white).

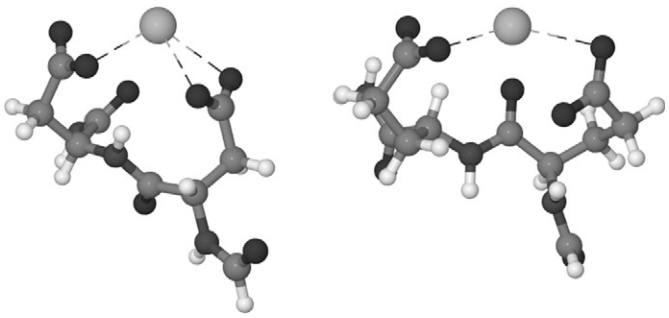

Fig. 3. Global minimum of calcium diaspartate, **1**, and calcium diglutamate, **2**, in the gas phase at the RI-MP2/SVP level of theory. The dotted lines indicate coordination between calcium and oxygen atoms. (Ca: light gray, O: black, N: dark gray, C: gray, H: white).

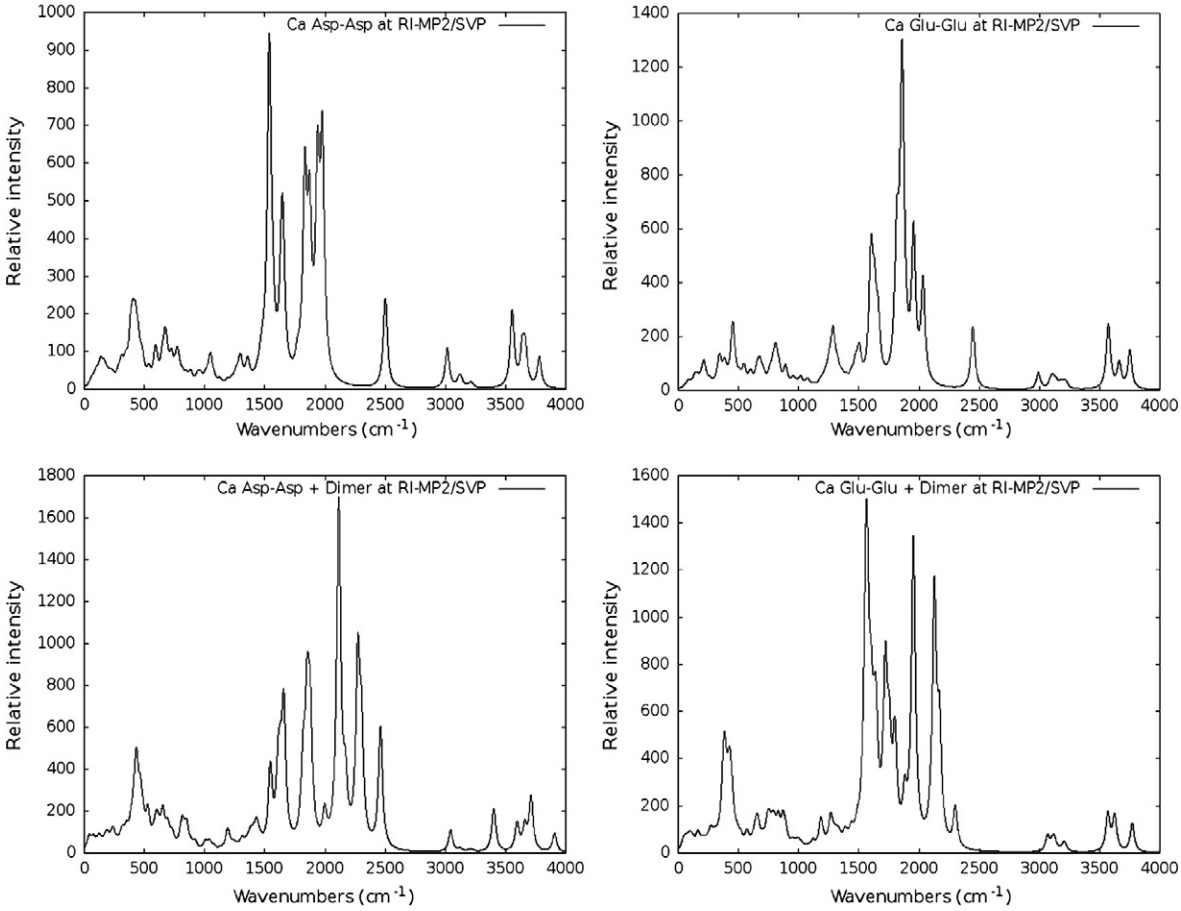

Fig. 4. Simulated IR spectra of calcium diaspartate (Ca Asp-Asp), calcium diglutamate (Ca Glu-Glu), calcium diaspartate-dimer (Ca Asp-Asp-dimer) and calcium diglutamate-dimer (Ca Glu-Glu-dimer) complexes, calculated in the gas phase at the RI-MP2/SVP level of theory.

All structural images were produced using Jmol [27]. Simulated IR spectra were generated by Molden [28]. The coordination sphere of calcium was considered up to 2.75 Å away from the center of the atom, according to the criteria set by Einspahr and Bugg [29].

2.1. MD conformational search for global minima of calcium dipeptides

Molecular dynamics yielded a very restricted set of conformers due to tight association of charges between calcium(II) and the carboxylates in vacuum, while using un-ionized carboxylates revealed mostly intramolecularly hydrogen-bonded conformers. To sample a larger fraction of the conformational space, we used the negatively charged dipeptide ion. From the resulting conformers, we generated two different structures by adding a calcium ion close to each side-chain carboxylate. Once the calcium ions were in place, all the structures were pre-optimized using the PM6 semiempirical Hamiltonian (to generate an adequate starting point for subsequent optimization), and then optimized at the RI-MP2/SVP level of theory.

2.2. Configurational search (blind-docking) for cluster-peptide optimum interaction

The general procedure is as follows: for each structure the program is fed (peptide and cluster), and the geometric centroid and the diameter of the circumscribing sphere are determined. The two structures are then moved in 3D space so that their centroids are a distance equal to the sum of the radii of both spheres (the spheres barely touch). Once the peptide and the cluster are in position, they are rotated around their own centroids a random number of degrees and the resulting structure is saved. 1000 configurations were generated in this way. These configurations were pre-optimized using PM6. Unique minima below 11.4 kcal/mol of relative energy were then optimized at the RI-MP2/SVP level of theory, and vibrational frequencies analyzed.

3. Results and discussion

The dynamics at the PM6 level revealed that the preferred conformation has both carboxylates coordinated to the calcium ion (see Fig. 2). None of the carbonylic oxygen atoms coordinate to the calcium.

Table 2
Conformational minima for calcium diglutamate in the gas phase at the RI-MP2/SVP level of theory. The total electronic energy includes thermal corrections and zero point energy from vibrational analysis.

Conformer	Total electronic energy (Eh)	Relative energy (kcal/mol)
6	−1791.65442	0.00
7	−1791.65041	2.52
8	−1791.64692	4.71
9	−1791.64536	5.68
10	−1791.64522	5.77
11	−1791.64518	5.80
12	−1791.64516	5.81
13	−1791.64334	6.95
14	−1791.64327	7.00
15	−1791.64320	7.04
16	−1791.64075	8.57
17	−1791.63989	9.12
18	−1791.63978	9.18

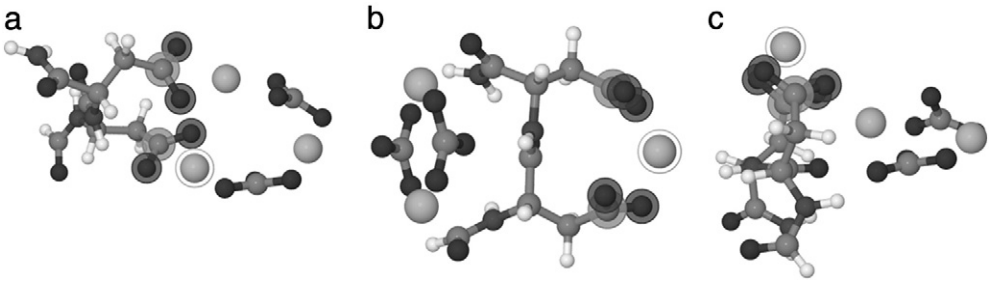

Fig. 5. Examples of calcium dimer bound to calcium diaspartate obtained by blind docking at the PM6 level. Structure (a) is the global minimum, (b) has a relative energy of 37 kcal/mol above the global minimum, while (c) has a relative energy of 40 kcal/mol above the global minimum. The atoms that form the active site are highlighted with halos. The highlighted calcium is the one that was originally part of the calcium diaspartate, prior to the addition of the calcium carbonate dimer. (Ca: light gray, O: black, N: dark gray, C: gray, H: white).

After re-optimization at the RI-MP2/SVP level in the gas phase, the global minimum for calcium diaspartate, **1** (see Table 1), has both carboxylate side-chains pointing towards the calcium ion. This conformer shows one instance of unidentate and one bidentate coordination to calcium. Although the carbonyl group in the C-terminus points towards the calcium, it is too far from it (2.84 Å > 2.75 Å Einspahr criterion) to be coordinated, yielding a coordination number of 3 (see Fig. 3).

The simulated IR spectrum (see Fig. 4) shows several salient peaks, namely, at 1536 (peptidic C – N stretch), 1649 (carboxylates asymmetric stretching), 1832 (peptidic C═O stretch), 1871 (carboxylate stretch on N-terminus side), 1938 (carboxylate stretch on C-terminus side), 1977 (C-terminus amide C═O stretch) and 2500 (N-terminus acyl C═O stretch) cm^{-1}.

Table 2 contains the relative energies for the conformations of calcium diglutamate that we found as energetic minima at the RI-MP2/SVP level of theory, with structure **6** as the global minimum. Coordination to the calcium is weak, as there are only two instances of unidentate coordination. Even though the peptidic carbonyl oxygen points towards the calcium, Ca – O distance is 2.87 Å, too far for coordination. There appears to be some hydrogen bonding between the C-terminus amide and one carboxylate on the side-chain.

The simulated IR spectrum of **6** (see Fig. 4) shows several salient peaks, namely, at 1600 (peptidic C – N stretch), 1662 (C-terminus amide C═O stretch), 1820 (carboxylates symmetric stretching), 1840 (N-terminus acyl C═O stretch), 1862 (carboxylate stretch on C-terminus side), 1957 (C-side carboxylate asymmetric stretch), 2035 (N-side carboxylate asymmetric stretch), and 2406 (peptidic C═O stretch) cm^{-1}.

The blind docking procedure evaluated the energies of the $CaCO_3$ dimer and the calcium dipeptides at a variety of orientations. The global minima show the dimer interacting with the carboxylates (see Figs. 5 and 6). Complexes with a coordinating amidic oxygen were found, as were complexes with the dimer away from the dicarboxylate–calcium moiety, but their energies were much higher than those interacting with the dicarboxylate–calcium. Thus, we consider the dicarboxylate–calcium moiety as the active site that recognizes a calcium carbonate dimer in both peptides.

In both diaspartate and diglutamate the global minima obtained for the dipeptide–dimer complex had the dimer interacting with the two carboxylates and the calcium (see Fig. 7).

Table 3 shows the relative energies for the minimum-energy configurations of the calcium diaspartate–$CaCO_3$ dimer complex calculated at the RI-MP2/SVP level of theory. The first, structure **19**, is the global minimum we found (see image on the left in Fig. 8).

Two of the calcium ions show double bidentate coordination, and the coordination number of the calcium ions is 4, either carboxylate–carbonate or carbonate–carbonate. The remaining calcium shows bidentate coordination to a carbonate and unidentate coordination to a carboxylate. There appears to be some hydrogen bonding between the peptidic amide and a side-chain carboxylate and between the C-terminus amide and a carbonate group. Vibrational analyses (see Fig. 4) show that the carbonyl bands are now spread apart. 1545 (peptidic C – N stretch), 1657 (CO_3^{2-} C═O stretch), 1818 (C-terminus C═O stretch), 1851 (mix of CO_3^{2-} and carboxylate stretches), 1876 (mix of CO_3^{2-} and N-terminus carboxylate stretch), 1997 (mix of CO_3^{2-} and C-terminus carboxylate stretch), 2114 (another mix of CO_3^{2-} and carboxylate stretches), 2272 (another mix of CO_3^{2-} and carboxylate stretches), 2302 (asymmetric carboxylate stretch with asymmetric CO_3^{2-} stretch), and 2460 (mostly carboxylate stretch, with some contribution from one CO_3^{2-}.)

From Table 4 we see the energies of the complexes calcium diglutamate–$CaCO_3$ dimer. The global minimum, **23**, shows three

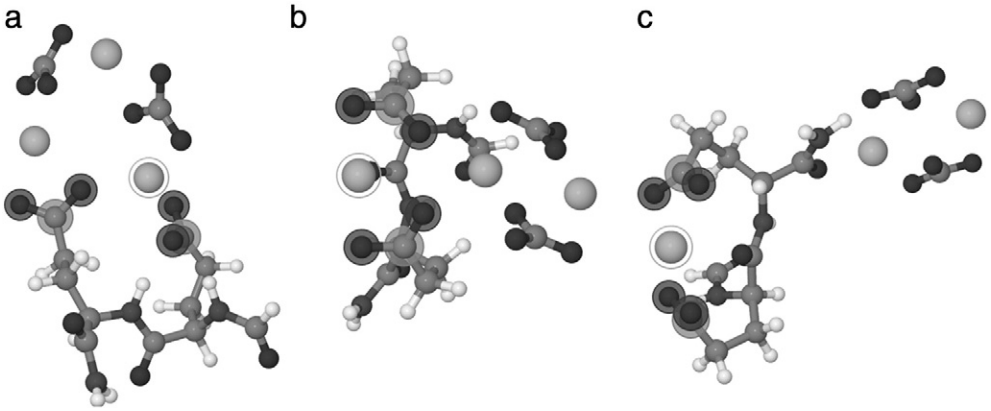

Fig. 6. Examples of calcium dimer bound to calcium diglutamate obtained by blind docking at the PM6 level. Structure (a) is the global minimum, (b) has a relative energy of 30 kcal/mol above the global minimum, while (c) has a relative energy of 40 kcal/mol above the global minimum. The atoms that form the active site are highlighted with halos. The highlighted calcium is the one that was originally part of the calcium diaspartate, prior to the addition of the calcium carbonate dimer. (Ca: light gray, O: black, N: dark gray, C: gray, H: white).

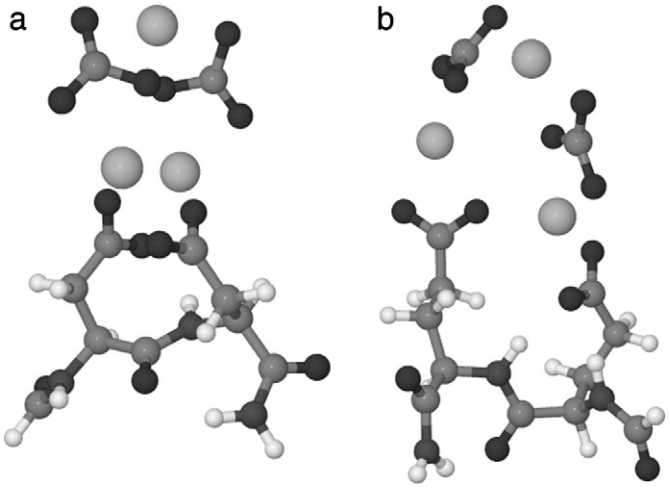

Fig. 7. Global minima of the complexes of (a) calcium diaspartate and (b) calcium diglutamate with $(CaCO_3)_2$ obtained by blind docking at the PM6 level. These are rotated and enlarged versions of the structures in Figs. 5a and 6a, respectively. (Ca: light gray, O: black, N: dark gray, C: gray, H: white).

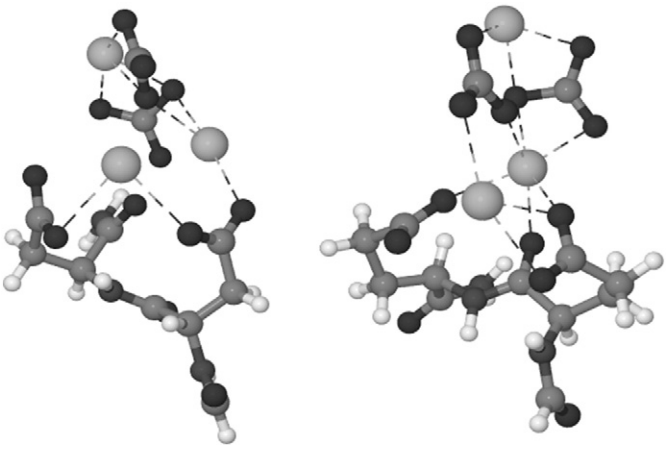

Fig. 8. Global minimum of the complexes calcium diaspartate–$(CaCO_3)_2$, **19**, (left) and calcium diglutamate–$(CaCO_3)_2$, **23**, (right) in the gas phase at the RI-MP2/SVP level of theory. The dotted lines indicate coordination between calcium and oxygen atoms (Ca: light gray, O: black, N: dark gray, C: gray, H: white).

instances of bidentate coordination and 5 instances of unidentate coordination. The coordination numbers of the calcium ions are 6, 3 and 3. The peptidic carbonyl oxygen participates in coordinating one calcium; this being the first low-energy structure with this feature. There appear some—possibly weak—hydrogen bonds, one between the N-terminus amidic proton and one side-chain glutamic oxygen and another between the peptidic carbonyl oxygen and a C-terminus amidic proton. Our vibrational analyses show that the C═O peaks due to the side-chain carboxylates shift upon binding to the cluster (see Fig. 4).

The calculated interaction energies (see Table 5) indicate that, in the gas phase, formation of the diaspartate–dimer complex, **19**, is favorable as it goes downhill in energy. On the other hand, formation of the diglutamate–dimer complex, **23**, is unfavorable, requiring an input of energy. This extra energy seems necessary to reorganize the structure of the dimer. In both cases, diaspartate and diglutamate, the initial structure before optimization had the dimer in its lowest-energy configuration. After the structural optimization, the structure of the dimer interacting with each dipeptide is distorted, as seen in Fig. 9.

Looking for the origin of this reorganization of the cluster, we observe that the greater distortion—with its concomitant energetic cost—happens in diglutamate (as seen in Fig. 9). The interaction of the dimer with diaspartate rearranges the structure, because of the spatial disposition of the carboxylates and the calcium in the peptide. It seems that the extra methylene group in the carboxylated side-chains in diglutamate gives rise to a less favorable ionic interaction in diglutamate than in diaspartate, therefore requiring a greater distortion of the dimer.

Because of all the preceding arguments, we propose that considerations of the carboxylate group as the "mineralizing glue" should be nuanced, as carboxylates belonging to different amino acids may show opposite affinities for binding calcium carbonate. These different interaction energies suggest that a strategic positioning of the diaspartate and diglutamate groups could direct aggregation of calcium carbonate units in a very finely-grained fashion, effectively acting as an organic *marshal*. *Organic marshaling* would be, then, the process by which a mineralizing protein directs aggregation of inorganic species towards energetically favorable sites in the protein—while avoiding unfavorable sites—by means of a specific spatial arrangement of its carboxylic groups, including both by sequence ordering and by higher-level structure.

This driving force of organic marshaling can be easily quantified as the difference in interaction energy between a favorable and an unfavorable site. So, from Table 5, the magnitude of the organic marshaling in the gas phase would be $24.1 - (-44.9) = 69$ kcal/mol, meaning that binding of a calcium carbonate dimer on a diaspartate site is 69 kcal/mol more favorable than binding to a diglutamate site.

All the previous considerations refer to the case in the gas phase. Given that biomineralization processes take place in aqueous media, consideration of aqueous solvation is in order. The high dielectric constant of water could in principle completely break the ionic structure of these complexes and separate the ions, so we decided to check for the effect of water using a continuum solvent model. We deem it sufficient to use a continuum solvent model, as we are only interested in the effect of the dielectric constant on the ionic bonds, and thus on the relative energies of both complexes. COSMO water solvation destabilizes both complexes, **19** and **23**, but the energy of interaction for **19** remains negative — meaning that it remains lower in energy than the separated diaspartate and calcium carbonate dimer in water. The relative strengths of the interaction energies remain practically unchanged, with **23** being much more unfavorable than **19**, both in the gas phase and in COSMO water. Under COSMO water, the effect of organic marshaling would amount to $75.4 - (-4.8) = 80.2$ kcal/mol, so even though water solvation may reduce the strength of binding, it seems to not reduce the strength of the organic marshaling.

Table 3
Conformational minima for calcium diaspartate–$(CaCO_3)_2$ complex in the gas phase at the RI-MP2/SVP level of theory. The total electronic energy includes thermal corrections and zero point energy from vibrational analysis.

Conformer	Total electronic energy (Eh)	Relative energy (kcal/mol)
19	−3592.87950	0.00
20	−3592.87801	0.93
21	−3592.87350	3.76
22	−3592.85939	12.62

Table 4
Conformational minima for calcium diglutamate–$(CaCO_3)_2$ complex at the RI-MP2/SVP level of theory. The total electronic energy includes thermal corrections and zero-point energy.

Conformer	Total electronic energy (Eh)	Relative energy (kcal/mol)
23	−3671.37728	0.00
24	−3671.37552	1.10
25	−3671.37375	2.22
26	−3671.37275	2.84
27	−3671.36896	5.22

Table 5
Interaction energies (kcal/mol) for calcium diaspartate and calcium diglutamate with a calcium carbonate dimer, calculated at the RI-MP2/SVP level of theory, both in the gas phase and with COSMO water. All the energies have been corrected for zero-point energy and BSSE.

	Aspartate	Glutamate
In the gas phase	−44.9	24.1
In water	−4.8	75.4

Fig. 9. Overlay comparing the structures of the calcium carbonate dimers. The original dimer before interaction with dipeptides is depicted in white, the dimer as complexed with diaspartate is gray, and the dimer complexed with diglutamate is black. The complexed dimers clearly are distorted, with respect to the original. The structures of the dipeptides were eliminated for clarity.

4. Conclusions

Our computational results indicate that recognition of a calcium carbonate dimer appears to require a specific spatial configuration of the calcium–dicarboxylate moiety, influenced by side-chain length. This, in turn, yields opposite energetics of recognition and binding between diaspartate and diglutamate. This suggests a new concept, *organic marshaling*, relevant for the mechanism of action of mineralizing proteins and probably helpful to protein designers.

Acknowledgments

We thank Programa de Apoyo a la Investigación Científica y Tecnológica (PAICyT) from Universidad Autónoma de Nuevo León for the financial support through grants CN067-09 and CE850-11. Thanks also to T. Daniel Crawford from the Chemistry Department at Virginia Tech for a generous allocation of computer time in the Cerebro supercomputing cluster. The authors also thank David Cantú-Morales for some preliminary calculations and one of the reviewers for posing helpful questions.

Appendix A. Supplementary data

Supporting information description: A pdf file with the optimized structures in XYZ format for all the species in the gas phase, with their calculated energies. This material is available free of charge via the Internet at figshare.com (http://dx.doi.org/10.6084/m9.figshare.1012860). Supplementary data to this article can be found online at doi: http://dx.doi.org/10.1016/j.bpc.2014.06.003.

References

[1] S. Weiner, Organization of extracellularly mineralized tissues: a comparative study of biological crystal growth, Crit. Rev. Biochem. Mol. Biol. 20 (1986) 365–408, http://dx.doi.org/10.3109/10409238609081998.
[2] S. Weiner, L. Hood, Soluble protein of the organic matrix of mollusk shells: a potential template for shell formation, Science 190 (1975) 987–989, http://dx.doi.org/10.1126/science.1188379.
[3] B.-A. Gotliv, N. Kessler, J.L. Sumerel, D.E. Morse, N. Tuross, L. Addadi, S. Weiner, Asprich: a novel aspartic acid-rich protein family from the prismatic shell matrix of the bivalve *Atrina rigida*, ChemBioChem 6 (2005) 304–314, http://dx.doi.org/10.1002/cbic.200400221.
[4] R.A. Metzler, I.W. Kim, K. Delak, J.S. Evans, D. Zhou, E. Beniash, F. Wilt, M. Abrecht, J.-W. Chiou, J. Guo, S.N. Coppersmith, P.U.P.A. Gilbert, Probing the organic-mineral interface at the molecular level in model biominerals, Langmuir 24 (2008) 2680–2687, http://dx.doi.org/10.1021/la7031237.
[5] P.U.P.A. Gilbert, M. Abrecht, B.H. Frazer, The organic-mineral interface in biominerals, Rev. Mineral. Geochem. 59 (2005) 157–185, http://dx.doi.org/10.2138/rmg.2005.59.7.
[6] L.W. Fisher, O.W. McBride, J.D. Termine, M.F. Young, Human bone sialoprotein: deduced protein sequence and chromosomal location, J. Biol. Chem. 265 (1990) 2347–2351.
[7] M.C. Kiefer, D.M. Bauer, P.J. Barr, The cDNA and derived amino acid sequence for human osteopontin, Nucleic Acids Res. 17 (1989) 3306, http://dx.doi.org/10.1093/nar/17.8.3306.
[8] J.P. Gorski, Acidic phosphoproteins from bone matrix: a structural rationalization of their role in biomineralization, Calcif. Tissue Int. 50 (1992) 391–396, http://dx.doi.org/10.1007/BF00296767.
[9] L.B. Gower, D.J. Odom, Deposition of calcium carbonate films by a polymer-induced liquid-precursor (PILP) process, J. Cryst. Growth 210 (2000) 719–734, http://dx.doi.org/10.1016/S0022-0248(99)00749-6.
[10] A. Chrissanthopoulos, E. Dalas, Semiempirical molecular orbital study of glycine solvation and of binding calcium carbonate on glycine polypeptides, J. Comput. Methods Sci. Eng. 7 (2007) 75–84.
[11] A. Navrotsky, Energetic clues to pathways to biomineralization: precursors, clusters, and nanoparticles, Proc. Natl. Acad. Sci. U. S. A. 101 (2004) 12096–12101, http://dx.doi.org/10.1073/pnas.0404778101.
[12] V.M. Rosas-García, I. Sáenz-Tavera, D. Cantú-Morales, Onset of amorphous structure in $CaCO_3$: geometric and electronic structures of $(CaCO_3)_n$ (n = 2–7) clusters by ab initio calculations, J. Clust. Sci. 23 (2012) 203–219, http://dx.doi.org/10.1007/s10876-011-0420-4.
[13] S. Mann, Molecular recognition in biomineralization, Nature 332 (1988) 119–124.
[14] C. Hetényi, D. van der Spoel, Efficient docking of peptides to proteins without prior knowledge of the binding site, Protein Sci. 11 (2002) 1729–1737, http://dx.doi.org/10.1110/ps.0202302.
[15] (a) G.M. Morris, D.S. Goodsell, R. Huey, A.J. Olson, Distributed automated docking of flexible ligands to proteins: parallel applications of AutoDock 2.4, J. Comput. Aided Mol. Des. 10 (1996) 293–304;
(b) G.M. Morris, D.S. Goodsell, R.S. Halliday, R. Huey, W.E. Hart, R.K. Belew, A.J. Olson, Automated docking using a Lamarckian genetic algorithm and an empirical binding free energy function, J. Comp. Chem. 19 (1998) 1639–1662.
[16] M. Clark, R.D. Cramer III, N. Van Opdenbosch, Validation of the general purpose TRIPOS 5.2 force field, J. Comp. Chem. 10 (1989) 982–1012.
[17] T. Hassinen, M. Peräkylä, New energy terms for reduced protein models implemented in an off-lattice force field, J. Comp. Chem. 22 (2001) 1229–1242.
[18] J.J.P. Stewart, Optimization of parameters for semiempirical methods V: modification of NDDO approximations and application to 70 elements, J. Mol. Model. 13 (2007) 1173–1213, http://dx.doi.org/10.1007/s00894-007-0233-4.
[19] J.J.P. Stewart, MOPAC2012 Stewart Computational Chemistry, Colorado Springs (USA), available at http://OpenMOPAC.net 2011.
[20] (a) D.E. Bernholdt, R.J. Harrison, Large-scale correlated electronic structure calculations: the RI-MP2 method on parallel computers, Chem. Phys. Lett. 250 (1996) 477–484;
(b) M.W. Feyereisen, G. Fitzgerald, A. Kormornicki, Use of approximate integrals in ab initio theory. An application in MP2 energy calculations, Chem. Phys. Lett. 208 (1993) 359–363;
(c) O. Vahtras, J. Almlöf, M.W. Feyereisen, Integral approximations for LCAO-SCF calculations, Chem. Phys. Lett. 213 (1993) 514–518.
[21] F. Weigend, R. Ahlrichs, Balanced basis sets of split valence, triple zeta valence and quadruple zeta valence quality for H to Rn: design and assessment of accuracy, Phys. Chem. Chem. Phys. 7 (2005) 3297–3305.
[22] F. Neese, The ORCA program system, Comput. Mol. Sci. 2 (2012) 73–78.
[23] A. Klamt, G. Schuurmann, COSMO: a new approach to dielectric screening in solvents with explicit expressions for the screening energy and its gradient, J. Chem. Soc. Perkin Trans. 2 (5) (1993) 799–805.
[24] E.F. Aziz, N. Ottosson, S. Eisebitt, W. Eberhardt, B. Jagoda-Cwiklik, R. Vácha, P. Jungwirth, B. Winter, Cation-specific interactions with carboxylate in amino acid and acetate aqueous solutions: X-ray absorption and ab initio calculations, J. Phys. Chem. B 112 (2008) 567–570, http://dx.doi.org/10.1021/jp805177v.
[25] I. Krossing, J.M. Slattery, C. Daguenet, P.J. Dyson, A. Oleinikova, H. Weingärtner, Why are ionic liquids liquid? A simple explanation based on lattice and solvation energies, J. Am. Chem. Soc. 128 (2006) 13427–13434, http://dx.doi.org/10.1021/ja0619612.
[26] F. Weigend, M. Häser, RI-MP2: first derivatives and global consistency, Theor. Chem. Accounts 97 (1997) 331–340, http://dx.doi.org/10.1007/s002140050269.
[27] Jmol — a chemical visualization program, http://www.jmol.org 2012.
[28] G. Schaftenaar, J.H. Noordik, Molden: a pre- and post-processing program for molecular and electronic structures, J. Comput. Aided Mol. Des. 14 (2000) 123–134.
[29] H. Einspahr, C.E. Bugg, The geometry of calcium carboxylate interactions in crystalline complexes, Acta Crystallogr. B 37 (1981) 1044–1052, http://dx.doi.org/10.1107/S0567740881005037.